6
Compression and Cochlear Implants

Fan-Gang Zeng

1. Introduction

Cochlear compression plays an important role in supporting the exquisite sensitivity, fine frequency tuning, and large operating dynamic range of the ear (Bacon, Chapter 1; Cooper, Chapter 2; Oxenham and Bacon, Chapter 3). With cochlear impairment, hearing threshold is elevated, and frequency selectivity and dynamic range are reduced (Bacon and Oxenham, Chapter 4; Levitt, Chapter 5). In cases of cochlear implants, the cochlear compression and other cochlear functions are bypassed altogether; hearing sensation is evoked by direct electric stimulation of the auditory nerve.

The goal of studying compression in cochlear implants is twofold. The first goal is practical. In a cochlear implant, all compression-related functions need to be replaced by a front-end artificial processor. The second goal is theoretical because direct stimulation of the auditory nerve provides a unique opportunity for studying the lack of cochlear compression in auditory perception, thereby complementing the studies in normal-hearing and cochlear-impaired listeners and allowing delineation of peripheral and central contributions to the functions of the overall system.

This chapter first briefly reviews how cochlear implants work (see Section 2). The psychophysical, or more precisely, psychoelectrical capabilities in cochlear implant users is reviewed, with an emphasis on the effect of loss of cochlear compression on perception (see Section 3). Section 4 contrasts the psychoacoustical and psychoelectrical data and discusses their inference on the theoretical models of auditory processing. Section 5 discusses practical issues on compression in cochlear implants in terms of restoring normal loudness growth, increasing electric dynamic range, and improving speech performance in implant users. Section 6 summarizes the current data and discusses future research directions.

2. Review of Cochlear Implants

2.1 Past and Present

When the Italian scientist Alessandro Volta invented the battery more than two centuries ago, one thing he did with his invention was to study how electric stimulation might affect sensations (Volta 1800). While studying the effects of electric stimulation on light, touch, smell, and other sensations, he placed one of two metallic probes in each ear and connected the ends of the probes to a 50-V battery. He observed that, ". . . at the moment when the circuit was completed, I received a shock in the head, and some moments after I began to hear a sound, or rather noise in the ears, which I cannot well define: it was a kind of crackling with shocks, as if some paste or tenacious matter had been boiling . . . The disagreeable sensation, which I believe might be dangerous because of the shock in the brain, prevented me from repeating this experiment . . ." It is believed that that was the first demonstration that electric stimulation can evoke hearing sensation.

At present, more than 50,000 people worldwide, including 10,000 children, have received cochlear implants. The earliest FDA-approved device was the House-3M single-electrode implant, with several hundred users. At present, there are three major cochlear implant companies, including the manufacturers of the Clarion device (Advanced Bionics Corporation, US), the Med-El device (Med-El Corporation, Austria), and the Nucleus device (Cochlear Corporation, Australia). An earlier multielectrode implant (the Ineraid device; Eddington et al. 1978) had a percutaneous plug interface and was ideal for many research purposes. In patients whose auditory nerve was sectioned by tumor removal, an auditory brainstem implant (ABI) has been used to stimulate the cochlear nucleus directly (e.g., Otto et al. 2002). The cochlear implant has evolved from the single-electrode device that was used mostly as an aid for lip reading and sound awareness to modern multielectrode devices that allow an average user to talk on the telephone. Despite the differences in speech processing and electrode design, there appears to be no significant difference in performance among the present cochlear implant users. The audiological criteria for having cochlear implantation has also relaxed, from bilateral total deafness (greater than 110 dB HL hearing loss) to severe hearing loss (greater than 70 dB HL) to the current suprathreshold speech-based criteria (less than 50% open-set sentence recognition with properly fitted hearing aids; NIH Consensus Statement 1995). More importantly, given the appropriate environment, most children who have received cochlear implants have shown language development parallel to that of normal-hearing children (Svirsky et al. 2000).

2.2 Design of a Cochlear Implant

In normal hearing, sound travels from the outer ear through the middle ear to the cochlea where the sound is converted into electric impulses that the brain can understand. Most cases with severe hearing loss involve damage to this sound-to-electric impulse conversion in the cochlea. A cochlear implant bypasses this natural conversion process by directly stimulating the auditory nerve with electric pulses.

Figure 6.1 shows a typical modern cochlear implant. First, a microphone picks up the sound (1) and sends it via a wire (2) to the speech processor (3) that is worn behind the ear or on a belt like a pager for older versions. The speech processor converts the sound into a digital signal according to the individual's degree of hearing loss. The signal travels back to the headpiece (4) that contains a coil transmitting coded radio frequencies through the skin (5). The headpiece is held in place by a magnet attracted to the

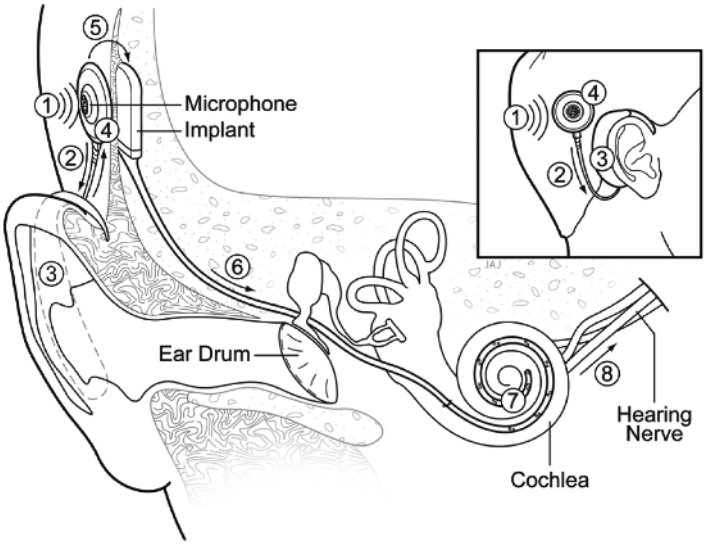

FIGURE 6.1. A typical cochlear implant system showing how it directly converts sound to electric impulses delivered to the auditory nerve. A microphone picks up the sound (1) and sends it via a wire (2) to a behind the ear speech processor (3). The processor converts the sound into a digital signal and sends the processed signal to a headpiece (4). The headpiece is held in place by a magnet attracted to the implant on the other side of the skin. Both the headpiece and the implant contain coils that transmit coded radio frequencies through the skin (5). The implant also contains hermetically sealed electronic circuits that decode the signals, convert them into electric currents, and send them along wires threaded into the cochlea (6). The electrodes at the end of the wire (7) stimulate the auditory nerve (8) connected to the central nervous system where the electrical impulses are interpreted as sound.

implant on the other side of the skin. The implant contains another coil receiving the radio frequency signal and also hermetically sealed electronic circuits. The circuits decode the signals, convert them into electric currents, and send them along wires threaded into the cochlea (6). The electrodes at the end of the wire (7) stimulate the auditory nerve (8) connected to the central nervous system, where the electrical impulses are interpreted as sound.

To a large degree, all modern multielectrode devices attempt to replicate the frequency analysis and amplitude compression mechanisms in acoustic hearing. They all divide a broadband audio signal (between several hundred hertz and 5–10 kHz) into 8–20 narrowband signals via analog or digital filters. However, they differ significantly in the postfiltering processing. One version of processing is to deliver the narrowband analog waveform to a tonotopically appropriate electrode that directly stimulates the auditory nerve. This type of processing has been called compressed analog (CA) or simultaneous analog stimulation (SAS) strategy (Eddington et al. 1978). Another version of processing is to extract the temporal envelope of the narrowband signals via rectification and low-pass filtering and then use the temporal envelope to amplitude modulate a fixed-rate biphasic pulse carrier. To avoid simultaneous stimulation between different electrodes, the pulses of the carrier between electrodes are systematically interleaved so that only one electrode will be stimulated at a time. When the number of analysis bands is the same as the number of electrodes, this nonsimultaneous processing is called continuous interleaved sampling (CIS) strategy (Wilson et al. 1991). However, when only a subset of the bands with maximal activities (e.g., 8 of the 22 electrodes) is stimulated, it is called the n-of-m (i.e., 8-of-20) or SPEAK strategy (McDermott et al. 1992). Recently, several combinations of these strategies have also become commercially available.

In addition to the common frequency analysis, all cochlear implants have adopted an amplitude compression scheme to match the wide acoustic dynamic range to the narrow electric range (see Section 3.1.1). The compression can be achieved with a gain control mechanism in the CA strategy, a logarithmic compression in the CIS strategy, or a power-function compression in the SPEAK strategy. Ideally, this compression scheme in cochlear implants can replicate the cochlear compression in acoustic hearing (see Section 4) and restore normal loudness growth (see Section 5).

2.3 Physiological Responses to Electric Stimulation

The cochlear implant bypasses all cochlear functions, including compression and synaptic transmission, to stimulate the auditory nerve directly. It is both important and interesting to compare the response of the auditory nerve to acoustic and electric stimulation so that we can understand the electrode-nerve interface and better appreciate the role of cochlear compression in perception. In the following paragraphs, the focus is on rate-intensity functions and phase-locking properties of auditory neurons.

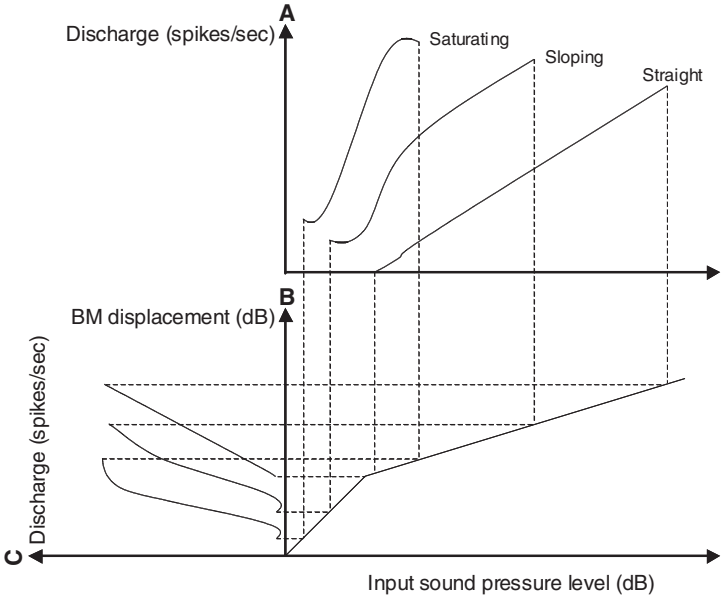

FIGURE 6.2. *A*: 3 typical types of rate-intensity functions for the auditory nerve fibers in acoustic hearing. Note the narrowest dynamic range in the saturating-type fiber and the widest dynamic range in the straight-type fiber. *B*: compressive input-output function of the basilar membrane (BM). *C*: Transformed "rate-intensity" functions in which the *x*-axis is the basilar membrane displacement. Note the uniformly narrow dynamic range in all 3 nerve fibers, suggesting that the acoustically observed different types of rate-intensity functions are mainly due to cochlear compression. (Adapted with permission from Yates et al. 1992. Copyright © 1992 Elsevier Science.)

Figure 6.2*A* shows three typical rate-intensity functions in acoustic hearing from the auditory neurons with high, medium, and low spontaneous activities (e.g., Sachs and Abbas 1974; Liberman 1978; Yates et al. 1990; Cooper, Chapter 2). Generally, the higher the spontaneous activity, the lower the response threshold and the wider the dynamic range. The dynamic range varies from 10 to 20 dB for high spontaneous rate neurons to 50 dB or more for low spontaneous rate neurons. In electric stimulation of a deafened ear, there is no spontaneous activity for the auditory neuron that has lost the dendritic connection to the inner hair cells (Kiang and Moxon 1972; Hartman et al. 1984; van den Honert and Stypulkowski 1984; Parkins and Colombo 1987). Although there are variations in electric thresholds, the dynamic range of the rate-intensity functions in electric stimulation is uniformly narrow and on the order of several decibels (Javel et al. 1987; Miller et al. 1999; Litvak et al. 2001).

Here it is demonstrated that the extremely narrow dynamic range in the rate-intensity function for electrical stimulation is a direct consequence of

the loss of cochlear compression. It has been argued (e.g., Sachs and Abbas 1974; Yates et al. 1992) that the difference in rate-intensity functions for acoustic stimulation reflects the compressive nonlinearity of the basilar membrane (Fig. 6.2*B*) rather than the neural response to the drive of the basilar membrane. For example, the straight rate-intensity function with a large dynamic range becomes surprisingly similar to the saturating function with a narrow dynamic range after taking the cochlear compression into account (Fig. 6.2*C*). Because the direct input to the neuron is the postsynaptic potential of the inner hair cell, we can consider Figure 6.2*C* as the response of the neuron to "electric stimulation" in a normal ear. Clearly, these "electrically stimulated" rate-intensity functions are more uniform and all have narrow dynamic ranges similar to what is observed in direct electric stimulation of the auditory nerve in a deafened ear.

Another example demonstrating the role of cochlear compression at the auditory nerve level is to compare the phase-locking abilities between acoustically and electrically stimulated auditory neurons. Because cochlear compression also contributes to the sharp frequency tuning in acoustic hearing, it must pose a physical limit to the phase-locking abilities of the auditory nerve according to the trade-off between frequency and time resolution. Figure 6.3 shows a synchronization measure as a function of

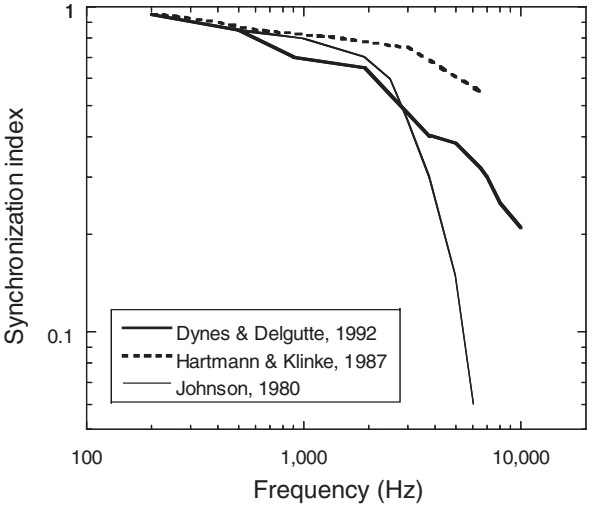

FIGURE 6.3. Synchronization index as a function of stimulus frequency in acoustic and electric stimulation. Note the sharply decreased synchronization in acoustic hearing (thin line) for frequencies above 1 kHz. In contrast, significant synchronization is still present at 6–10 kHz in electric hearing (dashed and thick lines). (Adapted with permission from Dynes and Delgutte 1992. Copyright © 1992 Elsevier Science.)

stimulus frequency with acoustic (Johnson 1980) and electric stimulation (Hartmann and Klinke 1987; Dynes and Delgutte 1992). Although the synchronization of firing decreases sharply for frequencies above 1,000 Hz in acoustic stimulation, a relatively high degree of synchronization is still maintained for frequencies as high as 10,000 Hz in electric stimulation. As seen in Section 4.3, the cochlear compression clearly limits normal-hearing listeners' ability to process temporal information.

2.4 Use of the Cochlear Implant to Probe Normal Auditory Processing

Although the cochlear implant has achieved a high level of medical success as a means of restoring partial hearing to deaf people, its use as a research tool to understand normal auditory processing is still underappreciated. This section shows how to use various patient populations in general and cochlear implant users in particular to understand normal auditory processing mechanisms.

We take an engineering reductionism approach that assumes that the function of the total system can be understood by assessing the function of each component. Figure 6.4 illustrates this approach. In auditory processing, the information is processed by the cochlea, then the auditory nerve, the cochlear nucleus, and, finally, other parts of the central nervous system and the feedback pathway from the central nervous system to the cochlea (the efferents). If we want to understand cochlear function, we can compare the performance between a normal-hearing listener and a cochlear implant user because in the latter case, the cochlea is bypassed and the auditory nerve is directly stimulated. Similarly, if we want to understand auditory nerve function, we can compare the performance between the cochlear implant user and an auditory brainstem implant (ABI) user because in the latter case, both the cochlea and the auditory nerve are bypassed and the cochlear nucleus is directly stimulated (Brackmann et al. 1993). The efferent function can also be inferred by comparing the performance between the ear with intact efferent innervation and the ear with sectioned efferents (Scharf et al. 1997; Zeng et al. 2000).

This approach certainly has its limitations. One limitation is the still poorly understood electrode-to-nerve interface that is likely not equivalent to the natural transducer-to-nerve synapses. Another limitation is the generally degenerated neurons (e.g., cell loss and demyelination) in cochlear implant users. These neural abnormalities may produce additional deficits other than what the lack of the cochlear mechanisms alone would cause. However, as a first approximation, it can be shown that this comparative and reductionism approach can reveal important processing mechanisms in auditory perception. The hope is that with better understanding of the biophysics and physiology of the system, we can delineate the peripheral versus

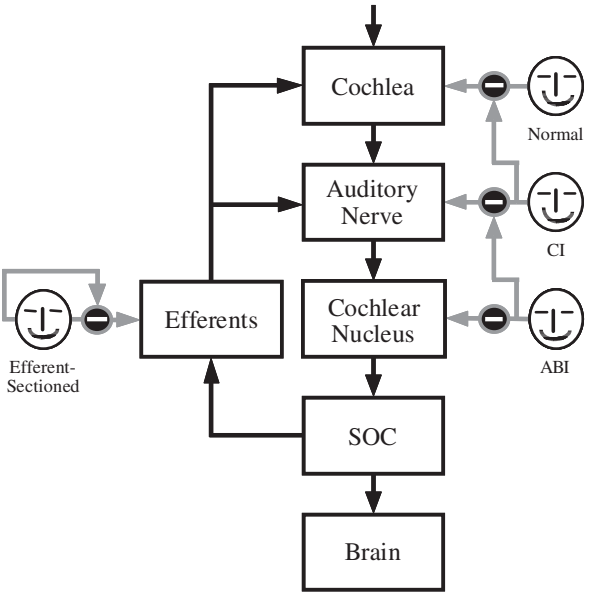

FIGURE 6.4. A reductionism model using hearing-impaired listeners to probe normal auditory functions. The blocks with downward arrows represent the auditory afferent pathway from cochlea to auditory nerve, cochlear nucleus, superior olivary complex (SOC), and the brain. The block with the upward arrow represents the auditory efferent pathway from SOC to the auditory nerve and cochlea. The happy faces represent normal-hearing, cochlear-implant (CI), auditory brainstem implant (ABI), and efferent-sectioned listeners. Because the cochlear implant bypasses the cochlea and directly stimulates the auditory nerve, a comparison between normal and CI listeners' performance will allow us to deduce the role of the cochlea in auditory processing. Similarly, a comparison between CI and ABI listeners will deduce the role of the auditory nerve and that between normal and efferent-sectioned listeners will deduce the role of efferents in auditory processing.

central contribution to the performance of the overall system. As a first step, the focus is on the cochlear implant users' psychoelectrical capabilities (Section 3).

3. Perceptual Consequences of Lost Cochlear Compression

Cochlear compression significantly affects auditory perception. This effect can be direct in terms of intensity processing or indirect in terms of frequency and temporal processing. This section demonstrates both the direct

and indirect effects of cochlear compression on auditory perception by examining perceptual performance in cochlear implant users.

3.1 Intensity Processing

A normal-hearing listener can process sound information with changes in intensity over 12 orders of magnitude, a 120-dB dynamic range in acoustic hearing (Bacon, Chapter 1). In addition, a normal-hearing listener can discriminate up to 200 intensity differences within this 120-dB dynamic range (Rabinowitz et al. 1976; Viemeister and Bacon 1988; Schroder et al. 1994). This remarkable dynamic range and its associated intensity resolution are deeply rooted in cochlear compression. Sections 3.1.1, 3.1.2, and 3.1.3 examine the changes in the dynamic range and intensity resolution caused by the loss of cochlear compression.

3.1.1 Dynamic Range in Electric Hearing

In electric hearing, the absolute threshold does not have the same meaning as in acoustic hearing. The acoustic threshold is limited to the minimal mechanical vibration that can be picked up by the hair cells and the nerve via an active mechanical mechanism (or amplifier). The electric threshold mostly reflects the type of electrode used, the electrode-tissue interface, the distance between the electrode and the nerve, and the degree and pattern of the nerve survival. Figure 6.5 presents dynamic range data as a function of frequency for both sinusoidal (left-slanted hatched areas) and pulsatile (right-slanted hatched areas) stimuli in eight cochlear implant users. The lower boundary of the dynamic range is the electric thresholds, and the upper boundary is the maximum acceptable loudness (Zeng and Shannon 1994, 1999).

Although there are significant individual differences in the absolute value of electric hearing thresholds and maximum loudness levels, the pattern of the data is clear and uniform. For sinusoids, both thresholds and maximum loudness levels increase monotonically as a function of frequency, whereas for pulses, both decrease monotonically as a function of frequency. The 100-Hz sinusoid produced the lowest threshold and the widest dynamic range (mean dynamic range = 30 dB), whereas the 100-Hz pulse produced the highest threshold and the narrowest dynamic range (mean dynamic range = 14 dB). The sinusoidal dynamic range decreases with frequency until 300–500 Hz as a result of a steeper increase in thresholds than in maximum loudness levels. On the other hand, the pulsatile dynamic range increases with frequency as a result of a steeper decrease in thresholds than maximum loudness levels. At 1,000 Hz, there is no statistical difference in dynamic range between sinusoidal (19 dB) and pulsatile (18 dB) stimuli. Both phenomenological (Shannon 1989a; Zeng et al. 1998b) and biophysical (Bruce

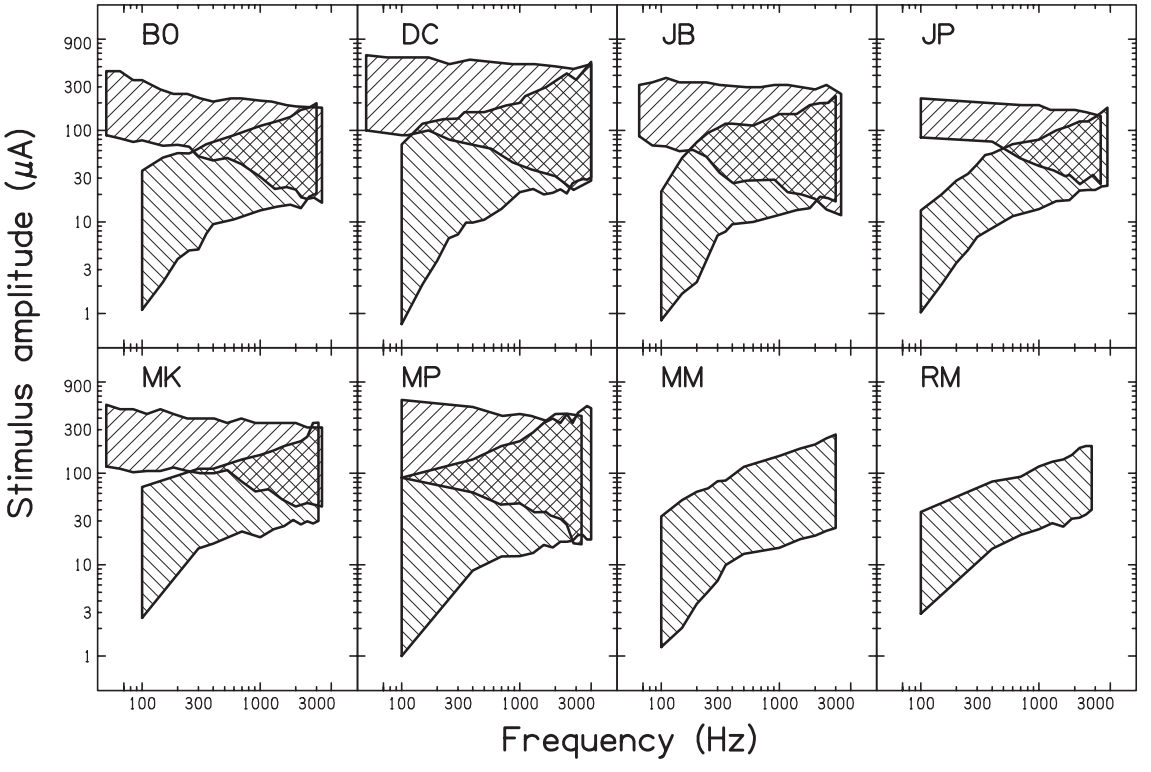

FIGURE 6.5. Dynamic range data as a function of frequency for sinusoidal (left-slanted hatched areas) and pulsatile (right-slanted hatched areas) stimuli in 8 Ineraid CI users. The lower boundary of the dynamic range is the electric threshold, and the upper boundary is the maximum acceptable loudness. All stimuli were 200 ms in duration. The pulsatile stimuli consisted of biphasic pulse trains of 100 ms/phase. The most apical electrode was stimulated in a monopolar mode. In contrast to the 100–120 dB acoustic dynamic range, the electric dynamic range varied between 10 and 30 dB (a ratio of 3 to about 30 between the maximum acceptable loudness and the threshold levels).

et al. 1999c) models have been developed to predict these dynamic range data.

3.1.2 Loudness Growth

How does loudness grow from threshold to maximal comfortable level? It has been well established in acoustic hearing that loudness grows as a power function of sound intensity with an exponent of roughly 0.3 (the famous Stevens' power law, Stevens 1961). In electric hearing, loudness growth has been modeled as either a power function or an exponential function (for a review, see Zeng and Shannon 1992).

There are generally two methods to obtain the loudness function. One method is to use loudness balancing to derive indirectly the loudness function of an unknown stimulus. For example, if we know that loudness (L) grows as a power function (f) of the intensity (I) for an acoustical stimulus [$L = f(I)$] and also know the balance function (g) between acoustic and electric (E) stimuli [$I = g(E)$], then we can easily derive the loudness function for the electric stimulus $\{L = f(I) = f[g(E)]\}$. This method has been used by a number of investigators (Eddington et al. 1978; Zeng and Shannon 1992; Dorman et al. 1993) and has produced the most convincing evidence for an exponential loudness function in electric hearing. Figure 6.6*A* shows a classic power function for loudness growth in the acoustic ear of a subject who had a brain stem implant on the other side. A brainstem rather than a cochlear implant user is used because (1) a complete set of loudness and just noticeable difference (JND) data is available for this subject (Fig. 6.6; see also Fig. 6.8) and (2) there is no difference in loudness growth between brainstem and cochlear implant users, at least for stimulus frequencies higher than 300 Hz (Zeng and Shannon 1994). Figure 6.6*B* shows a linear loudness balance function between linear electric amplitude (A) in microamperes and log acoustic amplitude in decibels ($E = a^*\log A$, where a is a constant). The linear function in these coordinates indicates that loudness grows as an exponential function in electric hearing

$$L = A^{\theta} = \left(10^{E/a}\right)^{\theta} = 10^{E\theta/a} \qquad (3.1.2.1)$$

Another method used to obtain loudness growth functions in electric hearing is via the classic magnitude estimation technique in which the subject has to report a number that (s)he believes corresponds to the loudness of the presented sound. Figure 6.7 shows such functions obtained by several investigators using the magnitude estimation method in cochlear implant users. The symbols are actual data, and the dashed lines represent exponential functions best fitted to the data. In some cases, a power function was found to provide as good (Fu and Shannon 1998) or better (Zeng and Shannon 1994) a fit to loudness growth for low-frequency (< 300 Hz) electric stimuli and can be directly compared to the expected 0.3 exponent or slope in normal-hearing listeners. However, it is sometimes

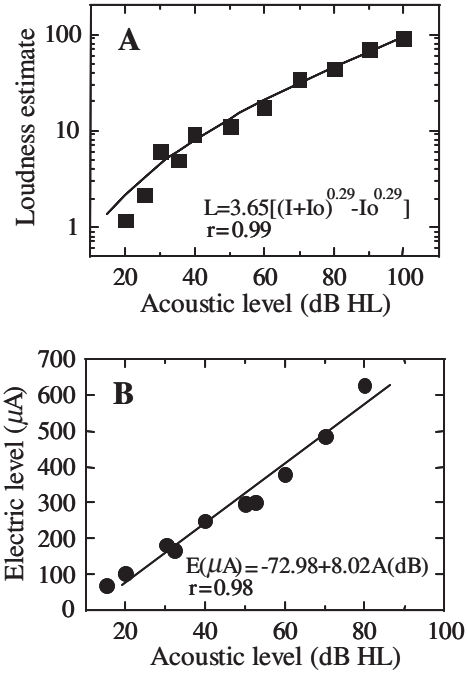

FIGURE 6.6. Loudness function in acoustic hearing (*A*) and loudness balance function between acoustic and electric hearing (*B*) in a listener who had normal hearing on 1 side and an ABI on the other side. The loudness function shows a typical power function with an exponent of 0.29 in acoustic hearing. Note the linear function in *B* in which the *x*-axis is in decibels for acoustic level, whereas the *y*-axis is linear microamperes for electric level, indicating a logarithmic loudness balance function between acoustic and electric hearing. (HL = Hearing Level)

difficult to use the power function to describe adequately the shallower loudness growth ("tail") near the threshold. The exponential loudness growth function can describe a wide range of stimulus conditions over the entire dynamic range (e.g., Chatterjee 1999; Chatterjee et al. 2000; McKay et al. 2001).

3.1.3 JND in Intensity

The intensity JND in electric hearing has been measured extensively (Bilger 1977; Eddington et al. 1978; Shannon 1983; Nelson et al. 1996; Zeng and Shannon 1999). Although the term intensity is used here to follow the general tradition in psychoacoustics (Viemeister and Bacon 1988), the actual unit used in electric hearing is usually current, a measure that is equivalent to pressure in acoustics. Here some interesting effects of the loss of cochlear compression on intensity discrimination in electric hearing are

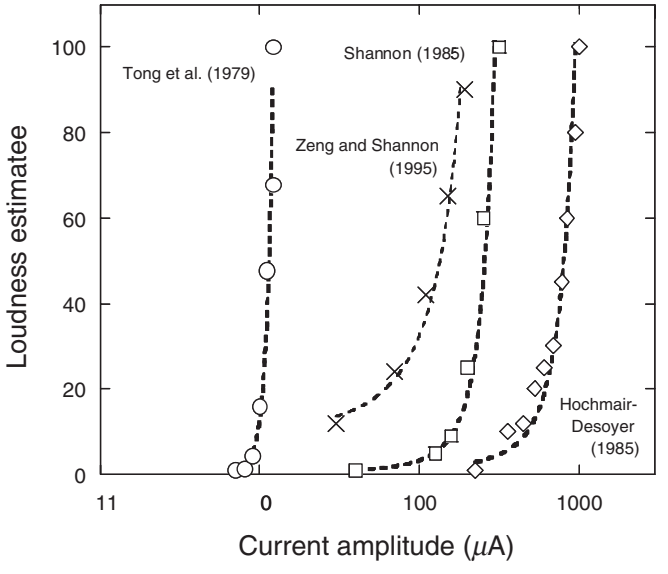

FIGURE 6.7. Loudness functions in electric hearing obtained from several previous studies. Dashed lines: fit to these data using an exponential loudness function in electric hearing. (All except for Zeng and Shannon (1995) are adpated with permission from Zeng and Shannon 1992. Copyright © 1992 Elsevier Science.)

demonstrated. Figure 6.8*A* shows the raw JND data (differences in microamperes as a function of standard level, also in microamperes) obtained in the same auditory brainstem listener whose loudness-matching data were shown in Figure 6.6. The JND in current was relatively constant at 70 μA within the lower half of the dynamic range (250–450 μA) but decreased monotonically to about 30 μA near the maximal comfortable loudness level. Because the overall dynamic range is about 500 μA, the JND size is relatively constant at about 10% of the dynamic range. In other words, the implant subject can resolve about 10 discriminable steps within the entire dynamic range. Similarly, results of 10–20 discriminable steps have been found in most cochlear implant subjects (Nelson et al. 1996; Zeng and Shannon 1999) in contrast to the 50–200 steps found in normal-hearing listeners (Rabinowitz et al. 1976; Viemeister and Bacon 1988; Schroder et al. 1994). If we use the total number of discriminable steps as the measure, then we can conclude that intensity discrimination abilities in cochlear implant users are much poorer than in normal-hearing listeners.

However, if we use a different measure of intensity discrimination, namely, the Weber fraction (the ratio between the absolute difference and the standard), as traditionally used in psychoacoustics, then we will reach a totally different conclusion. Figure 6.8*B* shows Weber fractions for both

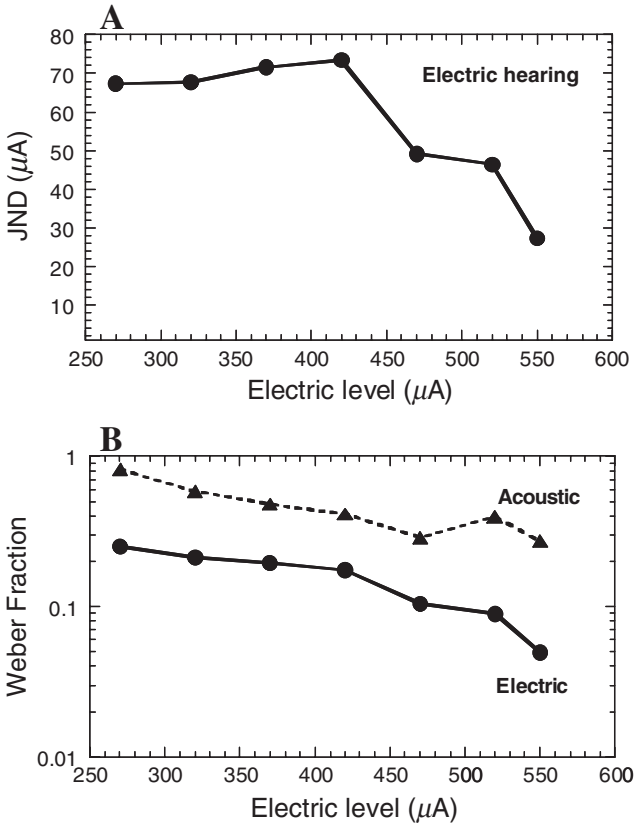

FIGURE 6.8. Intensity discrimination functions between acoustic and electric hearing in a listener who had normal hearing on 1 side and an ABI on the other side. *A*: just noticeable difference (JND) in absolute differences in electric hearing. *B*: JND in relative differences, i.e., the Weber fraction. For comparison, the acoustic Weber fractions measured from the same subject are plotted as a function of the electric currents (*x*-axis) that produced roughly the same loudness as the corresponding acoustic level (estimated from the loudness balance function shown in Fig. 6.6).

acoustic and electric hearing. The electric Weber fraction was obtained by dividing the values on the *y*-axis by their corresponding values on the *x*-axis in Figure 6.8*A*. The acoustic Weber fraction was calculated by converting the decibel difference (x) into the ratio between the pressure difference (ΔP) and the standard pressure (P), namely, $\Delta P/P = [10^{(x/20)}] - 1$. The acoustic Weber fraction is plotted as a function of the electric current that has produced roughly the same loudness as the corresponding acoustic level (estimated from the loudness balance function shown in Figure 6.6).

Figure 6.8*B* shows that the electric Weber fraction is almost an order of magnitude smaller than the acoustic Weber fraction throughout the entire

dynamic range (see also Nelson et al. 1996). As a matter of fact, we have often encountered cases where a cochlear implant user can reliably discriminate a loudness difference between 100 and 101 μA (e.g., Figs. 2 and 3 in Zeng and Shannon 1999). This 1% resolution is equivalent to a 0.08-dB level difference [20 log(1.01)], which is impossible to achieve with acoustic stimulation (the smallest difference is about 0.3–0.5 dB at 90–100 dB standard levels; e.g., Viemeister and Bacon 1988; Zeng et al. 1991). Thus, using the Weber fraction measure, we would reach the opposite conclusion that cochlear implant users have much better intensity discrimination abilities than normal-hearing listeners. The reason for reaching these apparent conflicting conclusions is largely due to the loss of cochlear compression in electric hearing (see Section 4.3). Although the electric JND is about one order of magnitude smaller than the acoustic JND, it does not necessarily result in a greater number of discriminable steps because the electric dynamic range is even more reduced by a factor of 4–5 orders of magnitude (20 vs. 100–120 dB).

3.2 Frequency Processing

3.2.1 Place Pitch

Because the cochlear compression is frequency selective, the sharp tuning that is normally observed in acoustic hearing is due in part to compression (Ruggero 1992). In electric hearing, the hope is to elicit tonotopic pitch perception by systematically stimulating the electrodes from apex to base in the cochlea. Unfortunately, despite equal physical distance between electrodes, pitch sensation evoked by these electrodes does not always conform to an orderly, perceptual relationship. Depending on electrode insertion depth, electrode configuration, nerve status, and other parameters, the pitch evoked by the same electrode array may have a different overall range and have a monotonic or nonmonotonic ("pitch reversal") relationship with the electrode array (Nelson et al. 1995; McKay et al. 1996; Collins et al. 1997; Busby and Clark 2000; Dawson et al. 2000). The spread of excitation as measured by forward-masking techniques has also been obtained in electric hearing (Lim et al. 1989; Cohen et al. 1996; Chatterjee and Shannon 1998). Although there is a greater spread of excitation from apical to basal electrodes, much like there is a greater spread of excitation from low to high frequencies in acoustic hearing (shown in Fig. 3.2 in Oxenham and Bacon, Chapter 3), no level dependence of the excitation pattern as would be observed as a consequence of nonlinear cochlear compression in acoustic hearing is observed in electric hearing.

3.2.2 Temporal Pitch

Because of better synchronization in electric hearing than acoustic hearing (Fig. 6.3), one might think that cochlear implant users can use timing cues

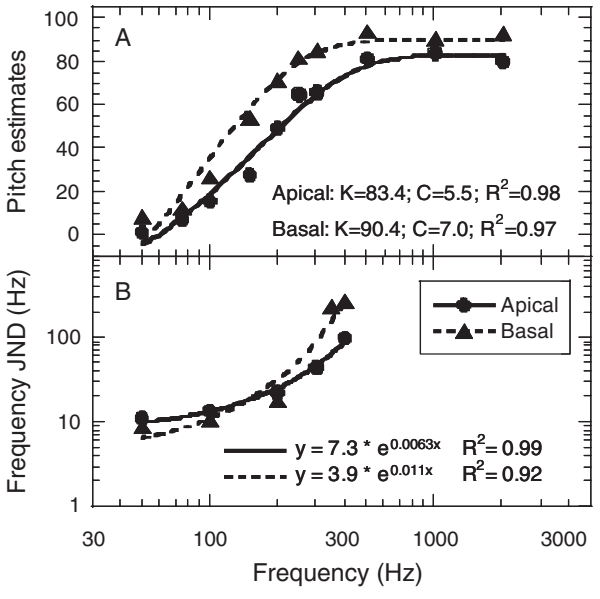

FIGURE 6.9. Pitch magnitude estimates (*A*) and JND (*B*) as a function of frequency in 1 Ineraid cochlear implant subject. Biphasic (100 or 200 ms/phase) pulses of different frequencies were used in the experiments. All stimuli were 300 ms in duration and delivered through a constant current source to the most apical (circles) or basal (triangles) electrode in a monopolar mode. Solid and dashed lines: predicted pitch functions from the frequency discrimination data (modeled as an exponential function; *B*). K, the saturation pitch value; C, constant perceptual difference in pitch (see Zeng 2002 for details).

to elicit more reliable and higher temporal pitch than normal-hearing listeners. Figure 6.9*A* shows pitch estimates as a function of frequency from both apical (circles) and basal (triangles) electrodes in one cochlear implant subject. Surprisingly, the pitch-frequency function saturates at roughly 300 Hz. The 300-Hz boundary has been consistently observed in all previous studies except for a few in which the implant users appeared to be able to use temporally based pitch up to 1 kHz (for a review, see Zeng 2002). Frequency JNDs (Fig. 6.9*B*) have also been measured to be relatively constant at 10–20 Hz for standard frequencies below 100 Hz but to increase drastically above that (see also Bilger 1977; Eddington et al. 1978; Shannon 1983; Townshend et al. 1987; Pijl and Schwarz 1995; McDermott and McKay 1997; Zeng 2002). These frequency JNDs are about one order of magnitude larger than the JNDs obtained with pure tones in normal listeners (Wier et al. 1977) but similar to those obtained with sinusoidally amplitude modulated noise in normal listeners (Formby 1985). These results suggest that the sharp frequency resolution observed in normal-hearing listeners is likely due to the place code rather than the temporal code.

3.3 Temporal Processing

The lack of cochlear compression significantly affects temporal processing in electric hearing. However, these effects are often masked in the literature. For example, gap detection and forward masking are perhaps the most frequently measured temporal processing tasks and have been found to be relatively normal in cochlear implant users (e.g., Bilger 1977; Eddington et al. 1978; Dobie and Dillier 1985; Preece and Tyler 1989; Shannon 1989b). We should be aware that these temporal measures are normal only after they are reorganized by some "normalized" intensity measures between acoustic and electric hearing (e.g., loudness or percent dynamic range). No one has explicitly studied whether the lost compression is the mechanism for the required "normalization" in forward masking in electric stimulation, but the lack of compression has been used to successfully account for the forward-masking data in cochlear-impaired listeners, particularly their slower recovery (Bacon and Oxenham, Chapter 4). Perhaps a temporal window model incorporating a compressive nonlinearity could reconcile the differences in forward masking observed between normal-hearing, cochlear-impaired, and cochlear implant users. Here three additional examples in temporal processing in which the lack of a compressive nonlinearity is clearly required and may not be readily masked by intensity normalization are discussed.

3.3.1 Temporal Integration

The first example is temporal integration. In acoustic hearing, for durations up to 100–200 ms, stimulus level can be traded almost linearly with its duration to achieve detection threshold. In other words, the slope of the temporal integration function [dB vs. log(time)] is about –3 dB per doubling of stimulus duration. It is unclear whether this represents, for example, one "look" at the output of a linear temporal integrator with a time constant of about 100–200 ms or multiple looks at the output of an integrator with a much shorter time constant (Oxenham and Bacon, Chapter 3). In electric hearing, temporal integration has been found to have a much shallower slope, albeit more variable than in acoustic hearing (Eddington et al. 1978; Shannon 1986; Pfingst and Morris 1993; Donaldson et al. 1997). Shannon (1986) found an average slope of –1.1 dB/doubling in 22 cases. Donaldson et al. (1997) found an average slope of –0.42/doubling, with a range from –0.06 to –1.94 dB/doubling, on 21 electrodes from 8 subjects. In addition, Donaldson et al. found that the slope of the temporal integration function tended to decrease with absolute threshold but increase with dynamic range. As seen in Section 4.3, this extremely shallow temporal integration function reflects mostly the lack of cochlear compression in cochlear implant users.

3.3.2 Amplitude Modulation Detection

The temporal modulation transfer function (TMTF) reveals a listener's ability to follow dynamic changes in amplitude and is represented by an amplitude modulation detection threshold [20 log(m)] as a function of modulation frequency (m is the modulation index). Figure 6.10 summarizes modulation detection from four different studies in acoustic and electric hearing. The bottom solid line in Figure 6.10 represents TMTF data obtained using a sinusoid to amplitude modulate a broadband noise carrier (Bacon and Viemeister 1985). The top solid line in Figure 6.10 represents the TMTF data obtained using a sinusoid to amplitude modulate a 5-kHz sinusoidal carrier (Kohlrausch et al. 2000). Amplitude modulation thresholds are also presented for cochlear implant users who detected modulation at a comfortable loudness level with either a pulsatile carrier (Fig. 6.10, open squares) or a sinusoidal carrier (Fig. 6.10, solid circles; from Shannon 1993).

All TMTF data show a low-pass characteristic function. The acoustic data with the noise carrier produce the lowest modulation sensitivity (–26 dB or

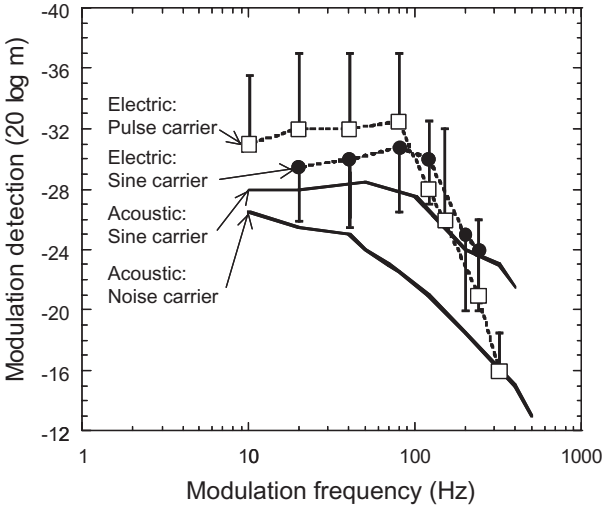

FIGURE 6.10. Temporal modulation transfer functions in acoustic hearing (noise and sinusoidal carriers) and in electric hearing (pulsatile and sinusoidal carriers). Open squares: data obtained using a sinusoid to amplitude modulate a pulse carrier in 7 Nucleus implant users; solid circles: data obtained using a sinusoid to amplitude modulate a sinusoidal carrier in 10 Ineraid implant users (Shannon 1993). Bottom solid line: acoustic temporal modulation transfer function (TMTF) data with the noise carrier (Bacon and Viemeister 1985); top solid line: TMTF with the 5-kHz sinusoidal carrier (averaged from Figs. 2 and 3 in Kohlrausch et al. 2000). Values are means ± SD.

5% modulation at 10 Hz) and 3-dB cutoff frequency (about 60 Hz), whereas the acoustic data with the sinusoidal carrier produce a somewhat higher sensitivity (–28 dB or 4% modulation) and cutoff frequency (about 170 Hz). The degraded performance with the noise carrier has been suggested to reflect the inherent fluctuations of the noise carrier, creating a modulation-masking situation (e.g., Kohlrausch et al. 2000; Moore and Glasberg 2001). Another possibility is that listeners may use an off-frequency listening cue, as evidenced by the presence of level-dependent modulation detection sensitivity with the sinusoidal carrier but the absence of it with the noise carrier. This off-frequency cue, particularly on the high-frequency side of the excitation pattern, tends to enhance the modulation due to the linear growth of excitation at these off frequencies.

The two sets of TMTF data in electric hearing have similar modulation sensitivities of about –30 dB (or 3% modulation) and cutoff frequencies at 150 Hz. These values are significantly better than the values obtained with the noise carrier but similar to those with the sinusoidal carrier in acoustic hearing. At least at an average level, these data suggest that it is more appropriate to use a sinusoid than a noise carrier to simulate modulation detection in electric hearing (which is not the case in the present simulation of cochlear implants; e.g., Shannon et al. 1995). On an individual basis, there is large variability with the modulation detection data in electric hearing, which has been shown to correlate with the productive use of temporal envelope cues in speech recognition (Cazals et al. 1994; Fu 2002). Moreover, the best modulation detection sensitivity reported in normal-hearing listeners was –37 dB (about 1.4% modulation; see Kohlrausch et al. 2000), but it is not unusual to find individual implant subjects who can detect 0.3–1.0% modulations (i.e., 20 log(m) = –50 to –40 dB; see Shannon 1992; Busby et al. 1993; Cazals et al. 1994; Chatterjee and Robert 2001; Fu 2002). This remarkable modulation sensitivity is at least partially due to the lack of cochlear compression and its perceptual consequences in electric stimulation.

3.3.3 Discrimination of Temporal Asymmetry

Patterson (1994a,b) produced “damped” and “ramped” sinusoids with asymmetrical temporal envelopes but identical long-term power spectra. The damped sinusoid is defined by three parameters: the sinusoidal carrier frequency, the exponentially damped temporal envelope (typically defined by the half-life time), and the repetition period of this exponentially damped envelope. The ramped sinusoid is simply the temporal reversal of the damped sinusoid. With an 800-Hz carrier frequency and 50-ms repetition period, Patterson found that normal-hearing listeners could typically discriminate the temporal asymmetry between damped and ramped sounds when the half-life of the envelope is between 1 and 50 ms. Under similar conditions, the cochlear implant users could discriminate between damped

and ramped sounds for half-lives as short as 0.5 ms and as long as 500 ms, an order of magnitude greater than the normal range (Lorenzi et al. 1997). Lorenzi et al. suggested that this superb performance in detecting temporal asymmetry in cochlear implant users is due to the lack of cochlear compression in electric stimulation. They further demonstrated this limiting role of cochlear compression in temporal processing by subjecting the implant listeners to listening to the damped and ramped sounds through their speech processors where there is an artificial amplitude compression circuit. As predicted, the implant users' ability to discriminate temporal asymmetry was greatly reduced to values that were within the normal range (1–24 ms; see Lorenzi et al. 1998).

4. Auditory Processing Revealed by Electric Hearing

Having reviewed selective behavioral responses to electric stimulation of the auditory nerve in cochlear implant users, what these psychoelectrical capabilities may tell us about the normal auditory processing mechanisms is now examined. Following the same outline as in Section 3, the auditory models inferred by electric hearing in intensity, frequency, and temporal processing are examined. Particular attention is paid to those mechanisms related to the lack of cochlear compression in cochlear implant users.

4.1 Intensity Processing

Here two issues in intensity processing are addressed. First, how does the auditory system encode the extremely large dynamic range in intensity? Second, can one derive the intensity-loudness function from the JND data in electric hearing? If so, what does it mean in terms of the role of the internal representation of intensity?

4.1.1 A Compression-Expansion Model for Loudness Coding

It has been known for a long time that loudness grows as a power function of intensity in acoustic hearing (Stevens 1961). Recent data have shown that loudness grows as an exponential function of intensity (or current) in electric hearing (see Section 3.1.2). Zeng and Shannon (1994) explored this difference in loudness growth between acoustic and electric hearing and proposed a general compression-expansion scheme for loudness coding in the auditory system. Figure 6.11 shows that the 100-dB dynamic range is first compressed in the cochlea to produce an output range of roughly 20 dB (Ruggero 1992). The narrowly compressed dynamic range is transmitted through the auditory nerve to the central auditory system and then expanded there to partially restore the large input range.

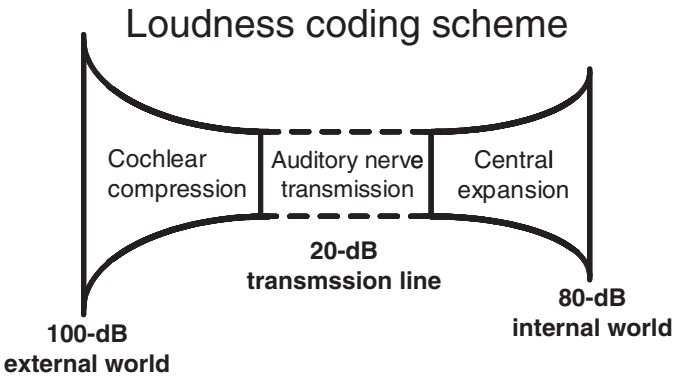

FIGURE 6.11. Compression-expansion model for loudness encoding. To solve the dynamic range problem between the large dynamic range in acoustic environments and the narrow dynamic range in neural transmission, the auditory system first compresses the acoustic dynamic range in the cochlea and then restores it by a central expansion. Similar coding schemes have been used in audio processing.

Mathematically, this compression-expansion coding for loudness can be approximately demonstrated by the following derivations (Fig. 6.12). Assume that N is the nerve output, then the cochlear compression can be approximated by

$$\mathrm{N} = a\log(\mathrm{I}). \tag{4.1.1.1}$$

The loudness is the product of the cochlear compression and the central expansion

$$\exp(\mathrm{N}) = \exp[a\log(\mathrm{I})] = \mathrm{I}^{a}. \tag{4.1.1.2}$$

We have thus obtained a power function describing the loudness and intensity relationship in acoustic hearing.

On the other hand, if the cochlear compression is bypassed as in the case of cochlear implants, then loudness is determined by only the central exponential process

$$\mathrm{L} = \exp(\mathrm{e}). \tag{4.1.1.3}$$

To further demonstrate this compression-expansion model of loudness coding, Zeng et al. (1998a) showed that one could obtain a good match to the power loudness function by exponentially expanding the measured compressive input-output function of the basilar membrane (e.g., Johnstone et al. 1986; Ruggero 1992). Zeng and Shannon (1994) suggested that this expansion occurs at the brainstem level. McGill and Teich (1995) further suggested a branching neural network as the explicit mechanism for expansion. On the other hand, Schlauch et al. (1998) showed that a similarly good

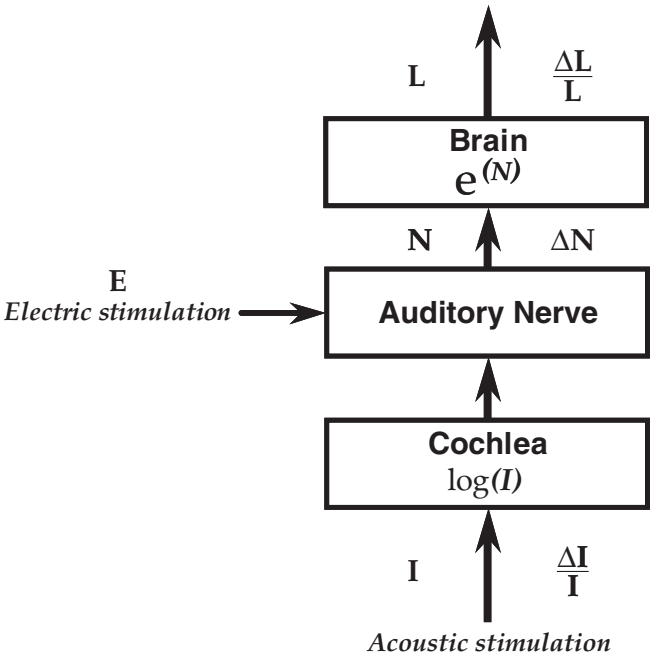

FIGURE 6.12. Unified model for intensity coding. On the left side of the block diagram, the sound intensity (I) is logarithmically compressed to drive the nerve, resulting in a neural discharge or count (N). This neural count is then exponentiated to result in a loudness percept (L). Such a compression-expansion model will give rise to a power loudness function in acoustic hearing. Bypassing the logarithmic compression, the electric stimulation results in the exponential loudness function. On the right side of the block diagram, the logarithmic compression and the exponential expansion transform from a constant relative difference in intensity ($\Delta I/I$) to a constant absolute difference in neural count (ΔN) and again to a constant relative difference in loudness ($\Delta L/L$).

match to the loudness function could be obtained by a presynaptic expansion mechanism: "squaring" the input-output function of the basilar membrane by the inner hair cells (for a further discussion of a square law nonlinearity, see Oxenham and Bacon, Chapter 3; Bacon and Oxenham, Chapter 4). Although the exact sites where expansion occurs are still debatable, note that this compression-expansion encoding scheme has been used frequently in audio engineering applications to overcome the narrow transmission channel problem (Furui 1988). It is not surprising that the sensory system has evolved with a similar mechanism for dealing with the dynamic range problem in the interface between the environment and the organism.

4.1.2 Loudness and the JND in Intensity

Another fundamental issue in psychophysics is whether the input-output function of the sensory system can be derived by its sensitivity measures. In this case, one would like to know whether the loudness function can be obtained by the intensity JND function. Fechner (1966) assumed that a stimulus JND (expressed as a Weber fraction or $\Delta I/I$) represents a constant unit in sensation ($\Delta L = I/I$). He integrated this equation and obtained his famous logarithmic law ($L = \log I$) in psychophysics. Although his logarithmic law was later replaced by a power law, his idea on the JND-loudness relationship still stimulates active research to this date (e.g., Houtsma et al. 1980; Zwislock and Jordan 1986; Viemeister and Bacon 1988; Schlauch et al. 1995; Allen and Neely 1997; Zeng and Shannon 1999; Hellman and Hellman 2001).

Zeng and Shannon (1999) formulated a unified framework that takes into account both the peripheral compression and central expansion and their relationship to the JND-loudness relationship (Figure 6.12). The peripheral compression converts a relative difference in intensity ($\Delta I/I$) into an absolute difference in neural count (ΔN), whereas the central expansion converts it back into a relative difference in sensation magnitude ($\Delta L/L$). The direct relationship between the relative differences in the stimulus and sensation domains has been called Brentano's law or Ekman's law (Ekman 1959; Stevens 1961).

In electric stimulation, neither Weber's law nor the near miss to Weber's law holds; rather, the absolute difference in microamperes or percent dynamic range is constant. Zeng and Shannon (1999) showed that the exponential loudness function can be directly derived by integrating the JND function in cochlear implant users. However, this simple relationship between the JND and loudness functions cannot be obtained in acoustic hearing, possibly due to the internal neural noise (i.e., spontaneous activity), multichannel listening, and compressive nonlinearity present in the normal-hearing listeners.

4.2 Frequency Processing

4.2.1 Pitch Models

Ruggero (1992) showed that cochlear compression and sharp frequency tuning are tightly coupled, and both probably reflect the nonlinear processing of the outer hair cells. With hearing impairment, the cochlea is more linear and both the compression and sharp tuning are reduced or lost (Bacon, Chapter 1; Cooper, Chapter 2; Bacon and Oxenham, Chapter 4). Electric stimulation of the auditory nerve in cochlear implant users reflects the extreme case of the loss of compression and sharp tuning. However, electric stimulation also provides an opportunity to test pitch models, which would be difficult, if not impossible, to do in acoustic stimulation.

One such example is to test the boundary and limit of temporal pitch in hearing. In acoustic stimulation, frequency changes always accompany changes in both the place of excitation and the phase locking of the nerve firing, making it difficult to assess the relative contribution of the place versus timing cues to pitch perception. The boundary of temporal pitch has been suggested to be at 1,500 Hz (Terhardt 1974) or 5,000 Hz, the frequency limit at which the auditory nerve stops to phase-lock to the stimulus (Johnson 1980). Burns and Viemeister (1976) used sinusoidally amplitude-modulated (SAM) noises to overcome this difficulty and found that only temporal cues could encode pitch up to about 500 Hz. However, the weak pitch the SAM noise evokes and the concern about the use of short-term spectral cues have made the results with SAM noise somewhat controversial and inconclusive for the boundary of temporal pitch.

With cochlear implants, the timing cue can be controlled totally independent of the place of stimulation. Surprisingly, virtually all studies of temporal pitch in cochlear implant users have shown that they cannot use temporal cues to form pitch perception for frequencies above 300–500 Hz (see Section 3.2.2). This psychophysical inability to encode temporal pitch above 300–500 Hz is in sharp contrast to the ability of the auditory nerve to phase-lock to electric stimuli up to 10,000 Hz (Fig. 6.3). This drastic difference between the psychophysical and physiological abilities in encoding temporal pitch in cochlear implant users may reflect the fact that the firing pattern due to electric stimulation is too artificially synchronous and the nerve is not totally healthy in the implant ears. However, the evidence from electric stimulation and the SAM noise in acoustic hearing strongly suggest that the brain may not use the timing cue above 300–500 Hz to encode pitch.

4.2.2 Pitch and the Frequency JND

Similar to the simple intensity JND-loudness relationship found in electric hearing, temporal pitch can be easily and reliably derived from frequency JND measures. Figure 6.9 shows that a simple integration of the frequency JND function can predict accurately the saturating temporal pitch function (Zeng 2002). The close couplings between the frequency JND and pitch and between the intensity JND and loudness in electric stimulation show that, without cochlear compression, the relationship between stimulus and sensation can be easily revealed. With the presence of the nonlinear compression, such a relationship is much more difficult to derive and describe in acoustic hearing. To test the generality of Fechner's (1966) classic hypothesis relating stimulus discriminability to sensation magnitude, we need to recognize and isolate the cochlear compression in this relationship.

4.3 Temporal Processing

The significant role of cochlear compression in temporal processing is not always apparent in traditional psychoacoustical studies because most tem-

poral models do not incorporate cochlear compression. By tweaking other parameters such as filter width, postfilter nonlinearity (rectification vs. power law), and decision variables and rules, these temporal models without compression can account for basic temporal phenomena such as temporal integration, gap detection, modulation detection, and forward masking (e.g., Viemeister 1979; Forrest and Green 1987; Moore et al. 1988; Oxenham and Plack 2000). More recently, however, compression has been implemented in the context of a temporal window model (see Fig. 3.5 in Oxenham and Bacon, Chapter 3). This model can account for a wide range of perceptual phenomena, including many aspects of temporal processing, as discussed in detail by Oxenham and Bacon (Chapter 3) and Bacon and Oxenham (Chapter 4). Here how the implant data (see Section 3.3) can reveal the role of compression in temporal processing is discussed.

First, the extremely shallow slope of the temporal integration function as observed in cochlear implant users can be readily modeled as a consequence of the loss of compression in these listeners. Yates et al. (1990) demonstrated that in acoustic hearing, the varieties and dynamic ranges of the rate-intensity functions in the auditory nerve reflect basilar membrane compression (Cooper, Chapter 2). Without the compression, the auditory nerve has a more uniform and steeper rate-intensity function in electric stimulation than acoustic stimulation. The steep rate-intensity function in electric hearing will result in a steep psychometric function as shown by both the experimental data (Donaldson et al. 1997) and a stochastic model of the electrically stimulated auditory nerve (Bruce et al. 1999a,b). Although Donaldson et al. (1997) used a multiple-looks model with a roughly 10-ms window to explain their data, Bruce et al. (1999c) found that the traditional "single-look" 100-ms integrator could also successfully explain the same data, suggesting that the lack of compression in electric hearing rather than the decision variable and rule is the critical factor determining the temporal integration function (see Bacon and Oxenham, Chapter 4, for a discussion of how a decrease in or loss of compression can influence temporal integration in acoustically stimulated hearing-impaired listeners).

Second, the lack of compression and filter ringing in electric stimulation can also account for exquisite sensitivity in intensity discrimination and detection of amplitude modulation and temporal asymmetry in cochlear implant users. A simple and parsimonious model detects the difference between peak and valley intensities. For example, implant listeners can detect amplitude modulations on the order of 1–5%, translating into 2–10% differences between the peak and the valley amplitudes [(minimum/maximum = (1 − m)/(1 + m)]. Similarly, for temporal asymmetry with a 500-ms half-life and 50-ms repetition period, the implant listener can detect about a 7% difference in amplitude between the beginning and the end of the temporal envelope [exp(–0.69*50/500)]. These differences in amplitude are consistent with the intensity discrimination directly mea-

sured in implant listeners at a comfortable loudness (i.e., Weber's fractions in the 1–10% range; see Nelson et al. 1996; Zeng and Shannon 1999; also Fig. 6.8).

Without evoking changes in the internal noise and other central decision variables in electric stimulation, the loss of cochlear compression alone can account for most of the difference in Weber's fraction between acoustic and electric stimulation. Except for the acoustic TMTF data with the sinusoidal carrier, normal-hearing listeners typically can detect intensity differences from 0.5 to 3 dB, translating into about a 6–40% difference in amplitude. This precompression difference, subject to a power function with an exponent of 0.3 (approximating the cochlear compression function; see Cooper, Chapter 2), is reduced to a postcompression difference of 2–11%, similar to the values typically found in cochlear implant users.

5. Practical Issues

Cochlear compression, or the lack of it with electric stimulation of the auditory nerve, significantly affects the design and performance of a cochlear implant. As seen in Section 3.1.1, the direct consequence of the lost compression is the extremely narrow dynamic range of 10–20 dB in cochlear implant users. The foremost important issue in the cochlear implant design is to fit speech sounds into this narrow dynamic range.

5.1 Automatic Gain Control and Instantaneous Compression

A normal-hearing listener can accommodate an extremely wide dynamic range of about 120 dB or an intensity change of over 12 orders of magnitude (Bacon, Chapter 1). The dynamic range of speech varies between 30 and 60 dB depending on the speech material, the acoustic measure [root mean square (rms) or envelope levels], and the definition of the speech dynamic range (for a review, see Zeng et al. 2002). All implants have an automatic gain control that adjusts the microphone sensitivity so that speech sounds, whether soft or loud, near or distant, can be optimally amplified to fit into a fixed 30–60 dB electric range that is compressed further to match the individual user's electric dynamic range. The automatic gain control tends to have a fast attack time (a few milliseconds) and a relatively slow release time (tens to hundreds of milliseconds; Levitt, Chapter 5).

On the other hand, the compression is instantaneous and typically accomplished by a lookup table in a digital implementation of the acoustic-to-electric amplitude-mapping process. Although the goal of this instantaneous compression is necessary because of the apparent mismatch in dynamic range between the environmental sounds and the electric stimu-

lation, it effectively partially recovers the function of the lost cochlear compression in cochlear implant users.

5.2 Restoring Normal Loudness Growth

One goal of the compression in cochlear implants is to restore normal loudness growth. Several researchers have shown a linear loudness-matching function between acoustic amplitude expressed in decibels and electric amplitude expressed in microamperes (Eddington et al. 1978; Zeng and Shannon 1992; Dorman et al. 1993; Fig. 6.6*B*). This linear function can be represented by

$$(20\log A - 20\log Ao)/(20\log Au - 20\log Ao) = a(E - T)/(U - T) + b \tag{5.2.1}$$

where Ao is acoustic threshold, Au is acoustic uncomfortable level, E is linear electric amplitude, T is electric threshold, U is electric uncomfortable level, and a and b are constants.

To restore normal loudness growth, the electric amplitude should then be determined by a logarithmic mapping function; in other words, a logarithmic compression from acoustic amplitude to electric amplitude is needed

$$E = 20\log(A/Ao)/IDR*(U - T)/a - b \tag{5.2.2}$$

where IDR is the input acoustic dynamic range. Applying the boundary conditions where E equals T when A equals Ao and E equals U when A equals Au, we have

$$E = 20\log(A/Ao)/IDR*(U - T) + T \tag{5.2.3}$$

Equation 5.2.3 shows that the ratio between electric dynamic range (U – T) and the IDR is a scaling factor, whereas T can be treated as a DC shift. Figure 6.13 illustrates such a mapping between IDR and electric dynamic range in cochlear implants. The x-axis (i.e., the IDR) determines the range of acoustic input mapped into the electric output range between threshold (T level) and the most comfortable loudness (M level). The speech processor first selects an acoustic level (0 dB on the x-axis) and maps it into an electric level (M level) that evokes the most comfortable loudness. The speech processor then maps either the 10-dB range below the 0-dB acoustic level into the audible electric dynamic range (the rightmost sloping line) or any other acoustic range into the same audible electric dynamic range. Presumably, any acoustic input level that is outside the IDR will be mapped into either a subthreshold electric level (less than T level) or a constant saturating level (greater then M level).

5.3 Speech Recognition

The choice of the acoustic dynamic range, the electric dynamic range, and the conversion from acoustic amplitude to electric amplitude can signifi-

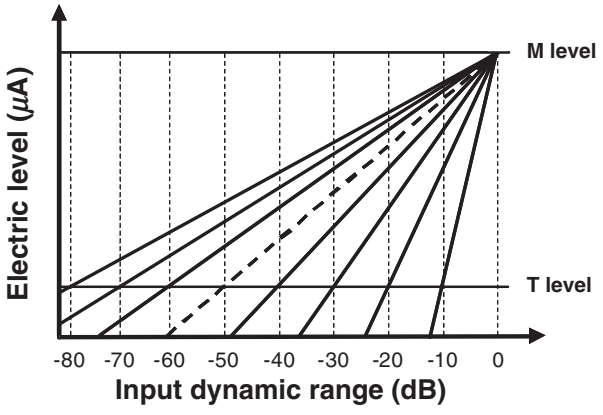

FIGURE 6.13. Logarithmic compression for acoustic-to-electric amplitude conversion in Clarion cochlear implants. The *x*-axis (i.e., the input dynamic range) determines the range of acoustic input mapped into the electric output range between threshold (T level) and the most comfortable loudness (M level). The speech processor first selects an acoustic level (0 dB on the *x*-axis) and maps it into an electric level (M level) that evokes the most comfortable loudness. The speech processor then maps either the 10-dB range below the 0-dB acoustic level into the audible electric dynamic range (the rightmost sloping line) or any other acoustic range into the same audible electric dynamic range. A 60-dB dynamic range map (dashed line) is typically set in the speech processor.

cantly affect speech performance in cochlear implant users. This section will examine each of these three factors in determining the cochlear implant performance and relate it to the psychophysical and theoretical aspects of auditory compression whenever appropriate.

5.3.1 Effect of IDR

Ideally, the IDR would be set to 120 dB so that the acoustic amplitude within this normal range is converted into a current value that evokes sensation between minimal and maximal loudness. Because of the narrow electric dynamic range and the limited discriminable steps within the range (about 10–20 dB dynamic range and 20 discriminable steps; see Nelson et al. 1996; Skinner et al. 1997b; Zeng et al. 1998b; Zeng and Galvin 1999; Zeng et al. 2002), the implant users might not be able to discern enough meaningful variations in sound intensity for the most important speech sound. Traditionally, speech dynamic range has been assumed to be 30 dB (e.g., Dunn and White 1940; ANSI 1969, 1997). Some of the earlier cochlear implants (e.g., Nucleus 22) have also set their IDR to this 30-dB value.

Using the standard logarithmic compression, Zeng et al. (2002) systematically examined the effect of adjusting the IDR on speech performance

in cochlear implant users. For consonants and vowels produced by multiple talkers, speech performance was optimal when the IDR was set at about 50 dB. The performance dropped off when the IDR was either decreased or increased. The optimal performance with a 50-dB IDR was consistent with the acoustically measured dynamic range for the temporal envelope distribution in these speech materials (Cosendai and Pelizzone 2001; Zeng et al. 2002).

5.3.2 Effect of Electric Dynamic Range

Clinicians spend most of the time during the programming of a cochlear implant trying to estimate the electric dynamic range as determined by the threshold and the maximum comfortable level. The threshold is usually called the T level, whereas the maximum comfortable level is called the M level or C level. Of course, we want to make sure that the acoustic information is mapped appropriately within the electric dynamic range; however, it is not clear how important an accurate measurement of this range needs to be to maintain a high level of speech performance in cochlear implant users.

Dawson et al. (1997) simulated errors in estimating the electric dynamic range by quasi-randomly reducing the maximum comfortable level by 20% from the actually measured values. They found a significant effect of this loudness imbalance on speech recognition, particularly in noise. Others (Skinner et al. 1997a; Zeng and Galvin 1999; Loizou et al. 2000a) also found similar effects of reducing the dynamic range on speech recognition, particularly again for vowels and in noise.

5.3.3 Effect of Compression

Several studies have systematically examined the effect of compression on speech performance in cochlear implant users (Fu and Shannon 1998, 2000; Zeng and Galvin 1999; Loizou et al. 2000b). In these studies, the degree of compression was varied from generally little compression to the steepest compression mimicking a step function. Although little or no compression generally produced the worst speech performance, the degree of compression had a relatively small effect on speech performance and depended on speech-processing strategies (Fig. 6.14). For example, Zeng and Galvin (1999) used the most compressive conversion from acoustic amplitude to electric amplitude, a step function that essentially converts variations of acoustic amplitude into a binary representation in electric amplitude. They found in cochlear implant users who used the SPEAK strategy that this extreme form of compression had relatively little effect on phoneme recognition in quiet. On the other hand, Fu and Shannon (1998) and Loizou et al. (2000b) showed in cochlear implant users using the CIS strategy that

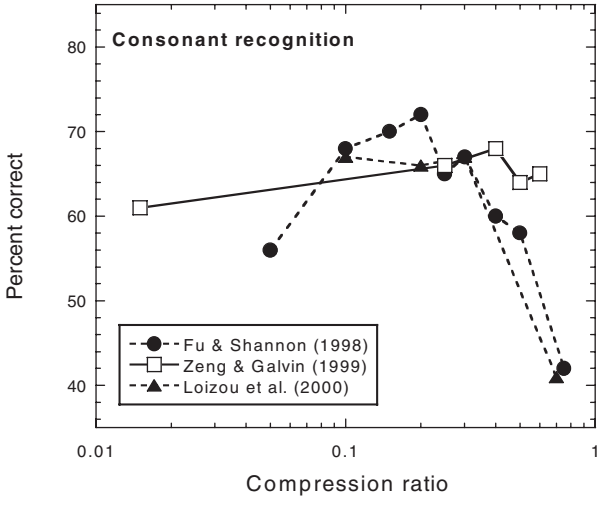

FIGURE 6.14. Consonant recognition as a function of compression ratios in cochlear implant listeners. The compression ratio is defined as the exponent (p) of a power function [$E = Eo + k(A - Ao)^p$], where Eo is the electric threshold, Ao is the minimal acoustic value to be mapped, and k is a constant. A logarithmic compression can be approximated by setting p to 0.3. The steplike compression in Zeng and Galvin (1999) is approximated by a compression ratio of 0.015 (the leftmost square).

the best speech performance was achieved when the compression restored normal loudness in cochlear implant users (with the compression ratio between 0.1 and 0.3). Additional benefits could also be obtained by selectively amplifying the low-value acoustic amplitudes in speech sounds (Geurts and Wouters 1999).

There is no question that compression needs to be restored by cochlear implants, but the question still remains regarding the form of the most effective compression. The preliminary data presented above show only a tip of the iceberg because, in reality, the best compression is not an isolated parameter but rather is one that interacts with other factors such as the listening environment (quiet vs. noise, speech vs. music), the processing strategies (temporal envelope vs. spectral features), and the electrode interactions (single- vs. multiple-electrode stimulation). For example, the popular strategy of extracting and coding the temporal envelope (Wilson et al. 1991) is more sensitive to the degree of compression than strategies of extracting the spectral features (Zeng and Galvin 1999). Ultimately, the compression has to be combined with the electrode-to-neuron interface to restore not only the normal loudness growth but, more importantly, the number of discriminable intensity steps as well as the range and resolution in frequency.

6. Summary

Using the cochlear implant to directly stimulate the auditory nerve has been proven to be an effective means of restoring partial hearing to deaf people. With today's modern multielectrode devices, an average implant user can talk on the telephone. We have begun to explore the utility and potential of the implant in probing basic auditory mechanisms, including cochlear compression. Overall, the basic research in cochlear implants is still in its infancy. It still remains a dream to incorporate compression in the cochlear implant to restore not only the loudness growth but also the number of discriminable steps in intensity, frequency tuning, and natural nerve response. This chapter has shown that the cochlear implant can be used as a powerful research tool to demonstrate the roles of cochlear compression in auditory functions.

(1) Cochlear compression plays an extremely important role in encoding the 120-dB dynamic range in acoustic hearing. Without this compression, the dynamic range is drastically reduced to 10–30 dB in electric hearing. The implant data suggest a general loudness-coding scheme consisting of a peripheral compression and a central expansion.

(2) Comparative studies between acoustic and electric hearing suggest that cochlear compression limits normal-hearing listeners' ability to discriminate differences in intensity and time (e.g., fast amplitude modulations and asymmetrical temporal changes). In this regard, the cochlear implant, sometimes referred to as the bionic ear, truly outperforms its natural counterpart.

(3) Employment of a nonlinear compression, similar to the natural cochlear compression, is important to restore normal loudness growth and improve perceptual performance in cochlear implant listeners. The exact form of compression and its interactions with processing, patient, and environmental factors still remain unclear.

Acknowledgments. I thank Ian Bruce, Gail Donaldson, Christian Lorenzi, and Roy Patterson for discussion on the role of compression in temporal processing, and Ackland Jones, Arthur Popper, and Sid Bacon for helpful comments on an earlier version of this chapter. Preparation of this manuscript was partially supported by National Institute on Deafness and Other Communication Disorders Grant R01-DC-02267-08.

References

Allen JB, Neely ST (1997) Modeling the relation between the intensity just-noticeable difference andloudness for pure tones and wideband noise. J Acoust Soc Am 102:3628–3646.

ANSI (1969) American National Standards Methods for the Calculation of the Articulation Index. ANSI S3.5-1969. New York: American National Standards Institute.

ANSI (1997) American National Standards Methods for the Calculation of the Speech Intelligibility Index. ANSI S3.5-1997. New York: American National Standards Institute.

Bacon SP, Viemeister NF (1985) Temporal modulation transfer functions in normal-hearing and hearing-impaired listeners. Audiology 24:117–134.

Bilger RC (1977) Psychoacoustic evaluation of present prostheses. Arch Otol Rhinol Laryngol 86:92–104.

Brackmann DE, Hitselberger WE, Nelson RA, Moore J, Waring MD, Portillo F, Shannon RV, Telischi FF (1993) Auditory brainstem implant. I. Issues in surgical implantation. Otolaryngol Head Neck Surg 108:624–633.

Bruce IC, Irlicht LS, White MW, O'Leary SJ, Dynes S, Javel E, Clark GM (1999a) A stochastic model of the electrically stimulated auditory nerve: pulse-train response. IEEE Trans Biomed Eng 46:630–637.

Bruce IC, White MW, Irlicht LS, O'Leary SJ, Dynes S, Javel E, Clark GM (1999b) A stochastic model of the electrically stimulated auditory nerve: single-pulse response. IEEE Trans Biomed Eng 46:617–629.

Bruce IC, White MW, Irlicht LS, O'Leary SJ, Clark GM (1999c) The effects of stochastic neural activity in a model predicting intensity perception with cochlear implants: low-rate stimulation. IEEE Trans Biomed Eng 46:1393–1404.

Burns EM, Viemeister NF (1976) Nonspectral pitch. J Acoust Soc Am 60:863–869.

Busby PA, Clark GM (2000) Pitch estimation by early-deafened subjects using a multiple-electrode cochlear implant. J Acoust Soc Am 107:547–558.

Busby PA, Tong YC, Clark GM (1993) The perception of temporal modulations by cochlear implant patients. J Acoust Soc Am 94:124–131.

Cazals Y, Pelizzone M, Saudan O, Boex C (1994) Low-pass filtering in amplitude modulation detection associated with vowel and consonant identification in subjects with cochlear implants. J Acoust Soc Am 96:2048–2054.

Chatterjee M (1999) Effects of stimulation mode on threshold and loudness growth in multielectrode cochlear implants. J Acoust Soc Am 105:850–860.

Chatterjee M, Robert ME (2001) Noise enhances modulation sensitivity in cochlear implant listeners: stochastic resonance in a prosthetic sensory system? J Assoc Res Otolaryngol 2:159–171.

Chatterjee M, Shannon RV (1998) Forward masked excitation patterns in multielectrode electrical stimulation. J Acoust Soc Am 103:2565–2572.

Chatterjee M, Fu QJ, Shannon RV (2000) Effects of phase duration and electrode separation on loudness growth in cochlear implant listeners. J Acoust Soc Am 107:1637–1644.

Cohen LT, Busby PA, Whitford LA, Clark GM (1996) Cochlear implant place psychophysics 1. Pitch estimation with deeply inserted electrodes. Audiol Neurootol 1:265–277.

Collins LM, Zwolan TA, Wakefield GH (1997) Comparison of electrode discrimination, pitch ranking, and pitch scaling data in postlingually deafened adult cochlear implant subjects. J Acoust Soc Am 101:440–455.

Cosendai G, Pelizzone M (2001) Effects of the acoustical dynamic range on speech recognition with cochlear implants. Audiology 40:272–281.

Dawson PW, Skok M, Clark GM (1997) The effect of loudness imbalance between electrodes in cochlear implant users. Ear Hear 18:156–165.
Dawson PW, McKay CM, Busby PA, Grayden DB, Clark GM (2000) Electrode discrimination and speech perception in young children using cochlear implants. Ear Hear 21:597–607.
Dobie RA, Dillier N (1985) Some aspects of temporal coding for single-channel electrical stimulation of the cochlea. Hear Res 18:41–55.
Donaldson GS, Viemeister NF, Nelson DA (1997) Psychometric functions and temporal integration in electric hearing. J Acoust Soc Am 101:3706–3721.
Dorman MF, Smith L, Parkin JL (1993) Loudness balance between acoustic and electric stimulation by a patient with a multichannel cochlear implant. Ear Hear 14:290–292.
Dunn HK, White SD (1940) Statistical measurements on conversational speech. J Acoust Soc Am 11:278–288.
Dynes SB, Delgutte B (1992) Phase-locking of auditory-nerve discharges to sinusoidal electric stimulation of the cochlea. Hear Res 58:79–90.
Eddington DK, Dobelle WH, Brackmann DE, Mladejovsky MG, Parkin JL (1978) Auditory prostheses research with multiple channel intracochlear stimulation in man. Arch Otol Rhinol Laryngol 87:1–39.
Ekman G (1959) Weber's law and related functions. J Psychol 47:343–352.
Fechner GT (1966) Elements of Psychophysics, Vol. I. Helmut E. Adler (trans). New York: Holt, Rinehart and Winston.
Formby C (1985) Differential sensitivity to tonal frequency and to the rate of amplitude modulation of broadband noise by normally hearing listeners. J Acoust Soc Am 78:70–77.
Forrest TG, Green DM (1987) Detection of partially filled gaps in noise and the temporal modulation transfer function. J Acoust Soc Am 82:1933–1943.
Fu QJ (2002) Temporal processing and speech recognition in cochlear implant users. Neuroreport 16:1635–1639.
Fu QJ, Shannon RV (1998) Effects of amplitude non-linearity on phoneme recognition by cochlear implant users and normal-hearing listeners. J Acoust Soc Am 105:2570–2577.
Fu QJ, Shannon RV (2000) Effects of dynamic range and amplitude mapping on phoneme recognition in Nucleus-22 cochlear implant users. Ear Hear 21:227–235.
Furui S (1988) Digital speech processing, synthesis, and recognition. New York: Marcel Dekker, pp. 139–204.
Geurts L, Wouters J (1999) Enhancing the speech envelope of continuous interleaved sampling processors for cochlear implants. J Acoust Soc Am 105: 2476–2484.
Hartmann R, Klinke R (1987) Impulse pattern in auditory-nerve fibers to extra- and intra-cochlear electrical stimulation. In: Banfai P (ed) Cochlear Implants: Current Situation, International Cochlear Implant Symposium. Duren, Germany, pp. 73–86.
Hartmann R, Topp G, Klinke R (1984) Discharge patterns of cat primary auditory fibers with electrical stimulation of the cochlea. Hear Res 13:47–62.
Hellman WS, Hellman RP (2001) Revisiting relations between loudness and intensity discrimination. J Acoust Soc Am 109:2098–2102.

Houtsma AJ, Durlach NI, Braida LD (1980) Intensity perception. XI. Experimental results on the relation of intensity resolution to loudness matching. J Acoust Soc Am 68:807–813.

Javel E, Tong YC, Shepherd RK, Clark GM (1987) Responses of cat auditory nerve fibers to biphasic electrical current pulses. Arch Otol Rhinol Laryngol 96:26–30.

Johnson DH (1980) The relationship between spike rate and synchrony in responses of auditory-nerve fibers to single tones. J Acoust Soc Am 68:1115–1122.

Johnstone BM, Patuzzi R, Yates GK (1986) Basilar membrane measurements and the traveling wave. Hear Res 22:147–153.

Kiang NY, Moxon EC (1972) Physiological considerations in artificial stimulation of the inner ear. Arch Otol Rhinol Laryngol 81:714–730.

Kohlrausch A, Fassel R, Dau T (2000) The influence of carrier level and frequency on modulation and beat-detection thresholds for sinusoidal carriers. J Acoust Soc Am 108:723–734.

Liberman MC (1978) Auditory-nerve response from cats raised in a low-noise chamber. J Acoust Soc Am 63:442–455.

Lim HH, Tong YC, Clark GM (1989) Forward masking patterns produced by intracochlear electrical stimulation of one and two electrode pairs in the human cochlea. J Acoust Soc Am 86:971–980.

Litvak L, Delgutte B, Eddington D (2001) Auditory nerve fiber responses to electric stimulation: modulated and unmodulated pulse trains. J Acoust Soc Am 110: 368–379.

Loizou PC, Dorman M, Fitzke J (2000a) The effect of reduced dynamic range on speech understanding: implications for patients with cochlear implants. Ear Hear 21:25–31.

Loizou PC, Poroy O, Dorman M (2000b) The effect of parametric variations of cochlear implant processors on speech understanding. J Acoust Soc Am 108: 790–802.

Lorenzi C, Gallego S, Patterson RD (1997) Discrimination of temporal asymmetry in cochlear implantees. J Acoust Soc Am 102:482–485.

Lorenzi C, Gallego S, Patterson RD (1998) Amplitude compression in cochlear implants artificially restricts the perception of temporal asymmetry. Br J Audiol 32:367–374.

McDermott HJ, McKay CM (1997) Musical pitch perception with electrical stimulation of the cochlea. J Acoust Soc Am 101:1622–1631.

McDermott HJ, McKay CM, Vandali AE (1992) A new portable sound processor for the University of Melbourne/Nucleus Limited multielectrode cochlear implant. J Acoust Soc Am 91:3367–3371.

McGill WJ, Teich MC (1995) Alerting signals and detection in a sensory network. J Math Psychol 39:146–162.

McKay CM, McDermott HJ, Clark GM (1996) The perceptual dimensions of single-electrode and nonsimultaneous dual-electrode stimuli in cochlear implantees. J Acoust Soc Am 99:1079–1090.

McKay CM, Remine MD, McDermott HJ (2001) Loudness summation for pulsatile electrical stimulation of the cochlea: effects of rate, electrode separation, level, and mode of stimulation. J Acoust Soc Am 110:1514–1524.

Miller CA, Abbas PJ, Robinson BK, Rubinstein JT, Matsuoka AJ (1999) Electrically evoked single-fiber action potentials from cat: responses to monopolar, monophasic stimulation. Hear Res 130:197–218.

Moore BC, Glasberg BR (2001) Temporal modulation transfer functions obtained using sinusoidal carriers with normally hearing and hearing-impaired listeners. J Acoust Soc Am 110:1067–1073.

Moore BC, Glasberg BR, Plack CJ, Biswas AK (1988) The shape of the ear's temporal window. J Acoust Soc Am 83:1102–1116.

Nelson DA, Van Tasell DJ, Schroder AC, Soli S, Levine S (1995) Electrode ranking of "place pitch" and speech recognition in electrical hearing. J Acoust Soc Am 98:1987–1999.

Nelson DA, Schmitz JL, Donaldson GS, Viemeister NF, Javel E (1996) Intensity discrimination as a function of stimulus level with electric stimulation. J Acoust Soc Am 100:2393–2414.

NIH Consensus Statement (1995) Cochlear implants in adults and children. Vol. 13, No. 2, pp. 1–30.

Otto SR, Brackmann DE, Hitselberger WE, Shannon RV, Kuchta J (2002) Multichannel auditory brainstem implant: update on performance in 61 patients. J Neurosurg 96:1063–1071.

Oxenham AJ, Plack CJ (2000) Effects of masker frequency and duration in forward masking: further evidence for the influence of peripheral nonlinearity. Hear Res 150:258–266.

Parkins CW, Colombo J (1987) Auditory-nerve single-neuron thresholds to electrical stimulation from scala tympani electrodes. Hear Res 31:267–285.

Patterson RD (1994a) The sound of a sinusoid: spectral models. J Acoust Soc Am 96:1409–1418.

Patterson RD (1994b) The sound of a sinusoid: time-interval models. J Acoust Soc Am 96:1419–1428.

Pfingst BE, Morris DJ (1993) Stimulus features affecting psychophysical detection thresholds for electrical stimulation of the cochlea. II. Frequency and interpulse interval. J Acoust Soc Am 94:1287–1294.

Pijl S, Schwarz DW (1995) Melody recognition and musical interval perception by deaf subjects stimulated with electrical pulse trains through single cochlear implant electrodes. J Acoust Soc Am 98:886–895.

Preece JP, Tyler RS (1989) Temporal-gap detection by cochlear prosthesis users. J Speech Hear Res 32:849–856.

Rabinowitz WM, Lim JS, Braida LD, Durlach NI (1976) Intensity perception. VI. Summary of recent data on deviations from Weber's law for 1000-Hz tone pulses. J Acoust Soc Am 59:1506–1509.

Ruggero MA (1992) Responses to sound of the basilar membrane of the mammalian cochlea. Curr Opin Neurobiol 2:449–456.

Sachs MB, Abbas PJ (1974) Rate versus level functions for auditory-nerve fibers in cats: tone-burst stimuli. J Acoust Soc Am 56:1835–1847.

Scharf B, Magnan J, Chays A (1997) On the role of the olivocochlear bundle in hearing: 16 case studies. Hear Res 103:101–122.

Schlauch RS, Harvey S, Lanthier N (1995) Intensity resolution and loudness in broadband noise. J Acoust Soc Am 98:1895–1902.

Schlauch RS, DiGiovanni JJ, Ries DT (1998) Basilar membrane nonlinearity and loudness. J Acoust Soc Am 103:2010–2020.

Schroder AC, Viemeister NF, Nelson DA (1994) Intensity discrimination in normal-hearing and hearing-impaired listeners. J Acoust Soc Am 96:2683–2693.

Shannon RV (1983) Multichannel electrical stimulation of the auditory nerve in man. I. Basic psychophysics. Hear Res 11:157–189.
Shannon RV (1986) Temporal processing in cochlear implants. In: Collins MJ, Glattke TJ, Harker LA (eds) Sensorineural Hearing Loss: Mechanisms, Diagnosis, Treatment. Iowa City, IA: University of Iowa Press, pp. 349–368.
Shannon RV (1989a) A model of threshold for pulsatile electrical stimulation of cochlear implants. Hear Res 40:197–204.
Shannon RV (1989b) Detection of gaps in sinusoids and pulse trains by patients with cochlear implants. J Acoust Soc Am 85:2587–2592.
Shannon RV (1992) Temporal modulation transfer functions in patients with cochlear implants. J Acoust Soc Am 91:2156–2164.
Shannon RV (1993) Psychophysics of electrical stimulation. In: Tyler RS (Ed) Cochlear Implants: Audiological Foundations. San Diego, CA: Singular Publishing Group Inc, pp. 357–388.
Shannon RV, Zeng FG, Kamath V, Wygonski J, Ekelid M (1995) Speech recognition with primarily temporal cues. Science 270:303–304.
Skinner MW, Holden LK, Holden TA (1997a) Parameter selection to optimize speech recognition with the Nucleus implant. Otolaryngol Head Neck Surg 117: 188–195.
Skinner MW, Holden LK, Holden TA, Demorest ME, Fourakis MS (1997b) Speech recognition at simulated soft, conversational and raised-to-loud vocal efforts by adults with cochlear implants. J Acoust Soc Am 101:3766–3782.
Stevens S (1961) To honor Fechner and repeal his law. Science 133:80–86.
Svirsky MA, Robbins AM, Kirk KI, Pisoni DB, Miyamoto RT (2000) Language development in profoundly deaf children with cochlear implants. Psychol Sci 11: 153–158.
Terhardt E (1974) Pitch, consonance, and harmony. J Acoust Soc Am 55:1061–1069.
Townshend B, Cotter N, Van Compernolle D, White RL (1987) Pitch perception by cochlear implant subjects. J Acoust Soc Am 82:106–115.
van den Honert C, Stypulkowski PH (1984) Physiological properties of the electrically stimulated auditory nerve. II. Single fiber recordings. Hear Res 14:225–243.
Viemeister NF (1979) Temporal modulation transfer functions based upon modulation thresholds. J Acoust Soc Am 66:1364–1380.
Viemeister NF, Bacon SP (1988) Intensity discrimination, increment detection, and magnitude estimation for 1-kHz tones. J Acoust Soc Am 84:172–178.
Volta A (1800) On the electricity excited by mere contact of conducting substances of different kinds. R Soc Philos Trans 90:403–431.
Wier CC, Jesteadt W, Green DM (1977) Frequency discrimination as a function of frequency and sensation level. J Acoust Soc Am 61:178–184.
Wilson BS, Finley CC, Lawson DT, Wolford RD, Eddington DK, Rabinowitz WM (1991) Better speech recognition with cochlear implants. Nature 352:236–238.
Yates GK, Winter IM, Robertson D (1990) Basilar membrane nonlinearity determines auditory nerve rate-intensity functions and cochlear dynamic range. Hear Res 45:203–219.
Yates GK, Johnstone BM, Patuzzi RB, Robertson D (1992) Mechanical preprocessing in the mammalian cochlea. Trends Neurosci 15:57–61.
Zeng FG (2002) Temporal pitch in electric hearing. Hear Res 174:101–106.
Zeng FG, Galvin JJ (1999) Amplitude compression and phoneme recognition in cochlear implant listeners. Ear Hear 20:60–74.

Zeng FG, Shannon RV (1992) Loudness balance between acoustically and electrically stimulated ears. Hear Res 60:231–235.
Zeng FG, Shannon RV (1994) Loudness-coding mechanisms inferred from electric stimulation of the human auditory system. Science 264:564–566.
Zeng, FG, Shannon RV (1995) Loudness of simple and complex stimuli in electric hearing. Ann Otol Rhinol Laryngol 104 (Suppl 166): 235–238.
Zeng FG, Shannon RV (1999) Psychophysical laws revealed by electric hearing. Neuroreport 10:1931–1935.
Zeng FG, Turner CW, Relkin EM (1991) Recovery from prior stimulation. II. Effects upon intensity discrimination. Hear Res 55:223–230.
Zeng FG, Shannon RV, Hellman WS (1998a) Physiological processes underlying psychophysical laws. In: Palmer A, Rees A, Summerfield AQ, Meddis R (eds) Psychophysical and Physiological Advances in Hearing. London: Whurr Publishers, pp. 473–481.
Zeng FG, Galvin JJ, Zhang CY (1998b) Encoding loudness by electric stimulation of the auditory nerve. Neuroreport 9:1845–1848.
Zeng FG, Martino KM, Linthicum FH, Soli SD (2000) Auditory perception in vestibular neurectomy subjects. Hear Res 142:102–112.
Zeng FG, Grant G, Niparko J, Galvin J, Shannon R, Opie J, Segel P (2002) Speech dynamic range and its effect on cochlear implant performance. J Acoust Soc Am 111:377–386.
Zwislocki JJ, Jordan HN (1986) On the relations of intensity jnd's to loudness and neural noise. J Acoust Soc Am 79:772–780.